Proceedings of ICMM 2005
3rd International Conference on Microchannels and Minichannels
June 13-15, 2005, Toronto, Ontario, Canada

ICMM2005-75126

REVIEW OF EXPERIMENTAL PROCEDURE FOR DETERMINING LIQUID FLOW IN MICROCHANNELS

A. D. Ferguson[1], M. Bahrami[2], and J. R. Culham[3]
Microelectronics Heat Transfer Laboratory,
Department of Mechanical Engineering,
University of Waterloo, Waterloo, ON, Canada N2L 3G1

Abstract

Large scatter in published experimental data has been observed with respect to classical theory. Recent data have confirmed that liquid, fully-developed, laminar flow in smooth microchannels of various cross-section is governed by the Navier-Stokes equations. However, when the dimensions of the channels are comparable with the wall roughness, surface effects become significant, as shown experimentally. To better assess the effect of surface phenomena such as wall roughness, sources of systematic bias must be eliminated. Some of the observed inconsistencies in data could originate from the experimental method. This paper explores and categorizes different approaches found in literature for measuring microflow characteristics and highlights the advantages and disadvantages inherent to these experimental techniques. A discussion of system components, experimental measurement and error analyses is included in the paper, with an emphasis on important issues which may have been overlooked in previous research. This study serves as a summary of experimental procedure and is a useful guideline for research in microfluidics. Moreover, several recommendations are proposed for improvement in areas requiring further study.

Nomenclature

A	=	channel area, m^2
D_h	=	hydraulic diameter, m, $\equiv \frac{4A}{P}$
f	=	Darcy friction factor
g	=	gravitational acceleration, m/s^2
h	=	liquid column height, m
K	=	pressure loss coefficient
L	=	channel length, m
Nu	=	Nusselt number
p	=	pressure, Pa
P	=	channel perimeter, m
Q	=	volumetric flow rate, m^3/s
R_a	=	average roughness, μm
Re	=	Reynolds number, $\equiv \frac{\rho V D_h}{\mu}$
V	=	flow velocity, m/s
z	=	measured value of surface heights, m

Greek

Δp	=	pressure drop, Pa
μ	=	absolute viscosity, $N \cdot s/m^2$
ρ	=	liquid density, kg/m^3
ω	=	absolute uncertainty

Subscripts

D_h	=	value measured using hydraulic diameter
e	=	entrance region

1 INTRODUCTION

A better understanding of thermal and hydrodynamic characteristics of flow in microchannels and microtubes is necessary as microfabrication has become widely used for

[1]Undergraduate Research Assistant, Microelectronics Heat Transfer Laboratory.
[2]Post-Doctoral Fellow, Department of Mechanical Engineering.
[3]Associate Professor, Director, Microelectronics Heat Transfer Laboratory. Member ASME.

microelectronic heat sinks, microfluidic devices and MEMS.

Much research has been undertaken to characterize microflow. Several research papers [1-4] have been published examining experimental work on microchannels. Large scatter is observed in the empirical data and no definitive conclusions can be drawn as to whether dimensional scale affects flow behaviour, or if conventional theory can be applied to microchannels. Recently, however, [5-7], conducted experiments in smooth channels of different cross-section, and concluded that the Navier-Stokes equations are valid for laminar flow in smooth microchannels.

A possible cause of some of the observed inconsistencies in data may be the experimental design and procedure. Indeed, Pfund et al. [8] found that in some analyses, researchers were attempting to compare their data with classical data for channels of *different* cross-sectional shape. It is thus evident that more research must be undertaken to further our knowledge in this field and to create consistent and coherent explanations of flow behavior.

This paper explores different techniques found in literature for measuring microflow characteristics, and highlights the advantages and disadvantages inherent to these experimental methods. A discussion of system component selection, experimental measurement and error analysis is included in the paper, with an emphasis on important issues which may have been overlooked in previous research. This paper serves as a summary of experimental procedures to date, and is a useful starting point for new research into microchannels.

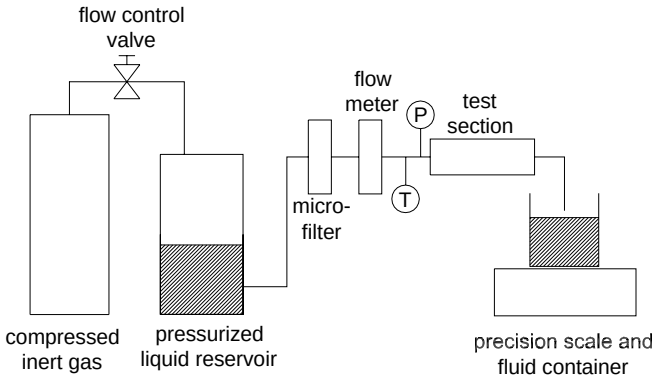

Figure 1. TYPE 1 : OPEN LOOP WITH COMPRESSED GAS

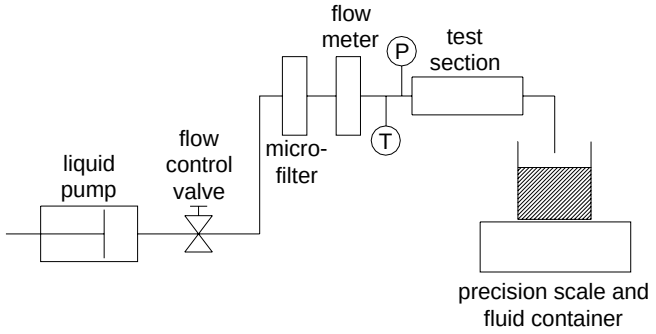

Figure 2. TYPE 2: OPEN LOOP WITH PUMP

2 APPARATUS

The experimental apparatus used to test microchannels can be grouped into one of three categories:

- Type 1: open loop system with compressed inert gas, Fig. 1
- Type 2: open loop system with a pump, Fig. 2
- Type 3: closed loop system, Fig. 3

Open loop systems are "once through" designs. The liquid is pressurized either by a compressed, inert gas or a pump. The liquid flows from the source, through a microfilter, into the test section and is then discharged to atmosphere. These systems are characterized by their relative simplicity and small number of components.

In closed loop systems, the liquid is pumped through a flow control, often one or more needle valves, microfilter, flow meter and then through the test section. The flow is recirculated into a liquid reservoir after it is returned to the test temperature via a heat exchanger and/or constant temperature bath.

Table 1 summarizes the experimental apparatus with the system type indicated in the first column. It is interesting to note the variety of channel sizes, $1.6 \leq D_h \leq 1900$, and shapes tested using a wide range of flow conditions, $8 \leq \mathrm{Re} \leq 23000$, where D_h and Re are defined as follows:

$$D_h = \frac{4A}{P}[m] \tag{1}$$

and

$$\mathrm{Re} = \frac{\rho V D_h}{\mu} \tag{2}$$

2.1 Pressure Source

Type 1 systems have a pressurized liquid reservoir (PLR) that contains the test liquid and a compressed inert gas, Fig. 4. All systems used compressed nitrogen gas except for Pfund et al. [8], who attached the PLR to a water main to supply both the test fluid and system pressure and used an in-line deionizing column to purify the water.

Type 2 and 3 systems are pressurized by a pump. For the open-loop systems, it is possible to run precision syringe

Table 1. EXPERIMENTAL APPARATUS SUMMARIES

Authors	System Type	Test Fluid	Channel Geometry	Channel Material	D_h (μm)	Re Range	fRe	Nu
Tuckerman & Pease [9]	-	deionized water	rect.	silicon	86-95	-		✓
Pfahler et al. [10]	1	n-propanol	rect.	silicon	1.6-76	-	✓	
Li et al. [11]	1	deionized water	circ.	glass, silicon, SS	79.9-205.3	300-2500	✓	
Zhang et al. [12]	2	deionized water	rect.	silicon	25-60	-	✓	✓
Chen et al. [13]	3	methanol	trap.	silicon	57-267	50-850	✓	✓
Kandlikar et al. [14]	2	distilled water	circ.	SS	620, 1032	500-3000	✓	✓
Celata et al.[15]	3	R114	circ.	AISI 316 SS	130	100-8000	✓	✓
Mala & Li [16]	2	deionized water	circ.	SS, fused silica	50-254	< 2500	✓	
Judy et al. [7]	2	water, methanol, isopropanol	sqr., circ.	SS, fused silica	15-150	8-1883	✓	
Gao et al. [17]	3	demineralized water	rect.	brass	40-49	200-8000	✓	✓
Liu & Garimella [5]	1	-	rect.	Plexiglas	244-974	230-6500	✓	
Wu & Cheng [6]	1	deionized water	trap.	silicon	25.9-291	13-2000	✓	
Peng et al. [18],[19]	3	water	rect.	SS	133-343	50-4000	✓	✓
Pfund et al. [8]	1	deionized water	rect.	polymer	253-1900	60-3450	✓	
Hsieh et al. [20]	2	deionized water	rect.	PMMA	146	< 1000	✓	
Xu et al. [21]	1	water	rect.	aluminum	46.8-344.3	20-4000	✓	
Owahib & Palm [22]	3	R134a	circ.	SS	800, 1200, 1700	1000-17000		✓
Adams et al. [23]	3	distilled water	circ.	copper	760, 1090	2600-23000		✓
Qu & Mudawar [24]	3	deionized water	circ.	copper	349	-	✓	✓

fRe: hydrodynamic characteristics are investigated
Nu: thermal characteristics are investigated

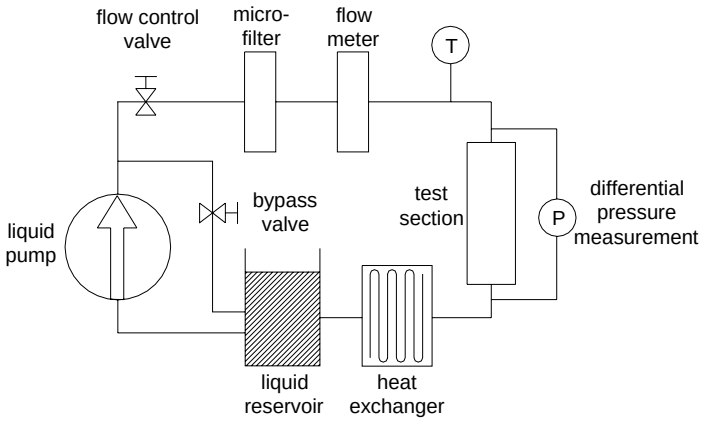

Figure 3. TYPE 3: CLOSED LOOP

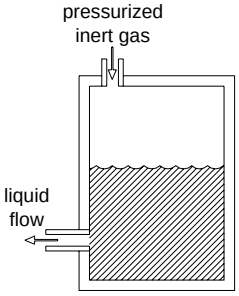

Figure 4. PRESSURIZED LIQUID RESERVOIR

pumps [7; 12] which have a fixed total supply volume before re-filling is required, but allow very precise flow rate control and provide a very high pressure, 16.2 MPa, [7].

Celata et al. [15] utilized a piston pump and Adams et al. [23] implemented a vane pump while [14; 22; 24] ran gear pumps. Notably, Liu and Garimella [5] also used a variable-flow gear pump initially but observed oscillations in the flow rate that created instability and affected flow transition and thus replaced the pump with a PLR.

2.1.1 Test Fluid. Table 1 shows the liquids tested in the reviewed literature. Water was predominantly used, often after being distilled or deionized. Deionized water can be made by replacing unwanted cations and anions or organic solids with harmless ions or with H^+ and OH^- which combine to form water molecules. Deionized water of lower purity can be made by reverse osmosis which involves using mechanical pressure to force water through a semi-permeable membrane that removes many ionic and

non-ionic particles.[4]

In comparison, distilled water will have less impurities than deionized water. However, distillers require significant cleaning and maintenance in order to keep the condensing surface free of impurities which may dissolve or mix into the newly-condensed water. Other sources of contamination of the condensed liquid in the distillation process include entrainment of other dissolvable gases and particles in unvapourized droplets transported by the water vapour.

2.2 Pressure Measurement

When examining the hydrodynamic behavior of a system, the most important measurement is the pressure drop across the test section. Determination of this parameter is required for calculation of the Darcy friction factor defined as:

$$f = \frac{2D_h \Delta p}{\rho L V^2} \tag{3}$$

and Reynolds friction factor product

$$f\,\mathrm{Re} = \frac{\pi}{2}\frac{D_h^4 \Delta p}{\mu L Q} \tag{4}$$

These parameters are used to compare data against classical theory. Uncertainty in pressure measurements are a function of the accuracy of the measurement device and the pressure losses due to inlet, outlet, and entrance length effects.

As previously mentioned, Type 1 and 2 systems are open to atmosphere at the test section outlet. Thus if the gauge pressure is measured at the test section inlet only, the total pressure drop across the test section can be easily determined [11; 12; 16]. The inlet and outlet losses must be accounted for when using this method.

Other researchers used pressure gauges, pressure transducers, or differential pressure transducers to measure pressure drop at the inlet and outlet of the specimen. More frequently, the pressure is tapped in the inlet and outlet manifolds, before the entrance and after the exit of the channel, respectively, if the channel is too narrow to install pressure probes in the channel itself, see Fig. 5.

2.2.1 Pressure Losses. The most common approach to account for pressure loss due to the inlet, outlet, and entrance effects was to utilize loss coefficients, K. The pressure drop was calculated as follows:

$$\Delta p = \frac{1}{2}\rho K V^2 \tag{5}$$

[4]Source: Water purification, Wikipedia The Free Encyclopedia, http://en.wikipedia.org/wiki/Water_purification

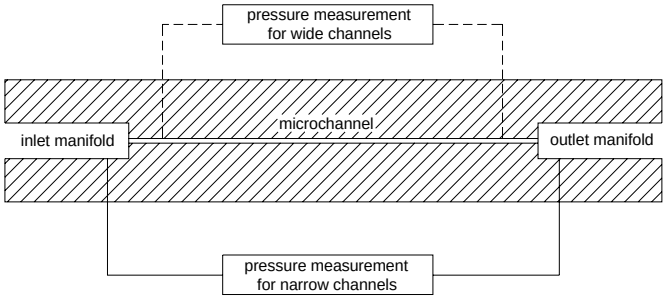

Figure 5. MICROCHANNEL PRESSURE MEASUREMENT

K values, based on conventional analytical and empirical data, can be found in [25], but little data are available for small scale applications. Thus the assumption must be made that mini and microscale flow behave similarly to the corresponding macroscale flow.

Pressure drop in the developing region is larger than that of the fully developed region and the entrance length is a function of D_h and Re for laminar flow [26]:

$$L_e \approx 0.06 D_h \,\mathrm{Re}_{D_h} \tag{6}$$

For example, at Re = 2300, the length of the developing region,L_e, is $138D_h$. Therefore, the contribution of the developing region must be considered in the total measured pressure drop. Alternatively, channel length must be selected based on the range of Reynolds number such that the developing region effect is negligible. In some cases, researchers such as [6; 21; 13] have used relatively short microchannels, L/D_h on the order of 100, at Re $>$ 2000, and did not consider this effect. The observed deviation from Hagen-Poiseuille theory, especially at high Re could be partially explained by developing region effects.

The reported K values from various authors are found in Table 2. [5; 19; 20; 24] accounted for pressure drops but did not indicate what K values and/or calculation methods were used. Wu and Cheng [6] used the same values given by Li et al. [11].

Liu and Garimella [5] and Pfund et al. [8] used sufficiently wide channels such that they were able to tap the pressure along the channel, eliminating the effects of the inlet and outlet.

Mala and Li [16] utilized another method to eliminate the effects of losses in pressure drop measurement. For each tube diameter, their experiments were performed with a short and long tube. Assuming inlet and outlet effects are independent of tube length, they were able to calculate pressure drop without these losses. For the shorter tube of length, L_1, a pressure drop, Δp_1, is measured. Similarly

Table 2. PRESSURE LOSS COEFFICIENTS

Authors	Inlet Coeff.	Outlet Coeff.	Other Coeff.
Li et al. [11]	1.5	-	0.66 (variation of momentum flux) 0.2 ('plump' velocity profile)
Chen et al. [13]	1.0	0.5	-
Judy et al. [7]	0.8	1.0	1.3 (hydrodynamic development length)
Gao et al. [17]	1.0	-	-

L_2 and Δp_2 are determined for the longer tube. For both microtubes, $\Delta p = \Delta p_2 - \Delta p_1$ and $\Delta L = L_2 - L_1$ giving the pressure drop, Δp, over the tube length ΔL. However, as mentioned above, the inlet and outlet pressure losses are proportional to V^2 and so V for both tubes must be equal in order to subtract the pressure drops. Mala and Li stated that the Δp is valid only for the same flow rate without reporting how the identical flow rates were achieved, but it can be assumed that they accounted for this factor in their experiment.

2.3 Flow Measurement

Volumetric flow rates were measured using an in-line flow meter or by collecting and measuring the volume of flow leaving the system over a period of time.

Turbine flow meters (also known as rotameters) were the most common type of in-line flow measurement [5; 8; 18]. Often, the flow meter was placed upstream of the test section and a microfilter was placed directly upstream of the flow meter to protect it and the test section from particles which might cause damage or inaccurate readings on the meter.

Judy et al. [7] measured the volumetric flow rate by measuring the flow until a minimum of 5 ml was collected in a graduated cylinder with a least count of 0.1 ml. This took a relatively long period of time, so they conducted tests to estimate the evaporation rates of the three test fluids to determine if liquid loss to the surroundings was significant. There was no detectable evaporation for water and methanol. Isopropanol, which is more volatile than the other two fluids, had a maximum of only 2.5% evaporation rate with respect to the slowest flow rate measured. Nonetheless, the collection container was capped with a vented stopper for all three test fluids to minimize evaporation. The liquid level in the graduated cylinder was maintained above the exit of the channel to eliminate losses due to surface tension. They found that the hydrostatic pressure of the fluid column

$$\Delta p_{hydrostatic} = \rho g h \tag{7}$$

was less than 0.05% of the minimum pressure difference across the microtube, and thus was negligible.

To determine the mass flow rate, the flow exiting the system was collected in a container, and was weighed by a precision scale. The flow rate was calculated by determining the rate of change of mass in the collection container with respect to time [5; 6; 11; 16].

2.4 Heat Transfer and Temperature Measurement

Many papers investigated the thermal performance of individual or banks of microtubes and channels for both single and multi-phase flow. In order to measure heat transfer coefficients or Nusselt numbers, Nu, it is necessary to know the inlet and outlet fluid temperatures and either the input energy into the test section, or the temperature of the test section walls.

Thermocouples (K or T type) were used in the majority of the reviewed literature. Typically, the thermocouples were located at the inlet and outlet manifolds of the microchannel test section. To measure temperature distribution along the channel length, thermocouples were attached to the outside or buried in the microchannel wall, depending on the size of the housing.

In order to heat the test sections for thermal testing, [13; 14; 18; 22] utilized electrical resistance, and supplied DC voltage across the specimen itself.

Gao et al. [17] and Qu and Mudawar [24] designed the housing to incorporate cartridge heaters and Adams et al. [23] used band heaters which surrounded a cylindrical test section.

Tuckerman and Pease [9] used thin-film WS_2 resistors which were sputter coated to a thickness of 1 μm onto the channel outer surface. Zhang et al. [12] utilized temperature-sensitive resistors to heat the specimen, and by measuring the voltage supplied to the resistor, it was possible to determine the resistor temperature and thus the wall temperature at that location.

Celata et al. [15] heated a bank of six microtubes, connected to common inlet and outlet headers, by condensing water vapor on the test section. By measuring the vapour pressure of the water, and finding the corresponding saturation temperature, they indirectly measured the temperature of the tubes without attaching any external bodies that may have influenced the wall temperature.

Another issue which has not drawn much attention in literature is the effect of viscous heating. With the relatively large pressure drops found at small flow rates, a large amount of kinetic energy is converted into heat. Judy et al. [7] were the only authors to report this phenomenon, finding that in some cases the fluid temperature from inlet to outlet increased by as much 6 °C. The variation in temperature implies that liquid properties are not constant along the channel length and this variation must be considered in

Table 3. ROUGHNESS ESTIMATES

Authors	Reported Roughness
Chen et al. [13]	$R_a = 0.1\ \mu m$
Kandlikar et al. [14]	$R_a = 1.0\text{-}3.0\ \mu m$
Mala & Li [16]	$R_a = 1.75\ \mu m$
Gao et al. [17]	$R_a < 0.1\ \mu m$
Pfund et al. [8]	$R_a = 0.09\text{-}1.90\ \mu m$
Hsieh et al. [20]	$R_a = 0.6\ \mu m$
Li et al. [11]	$\epsilon = \begin{cases} \text{glass, silicon:}<0.1\% \\ \text{SS:3-4\%} \end{cases}$
Liu & Garimella [5]	$\epsilon < 3\%$
Wu & Cheng [6]	$\epsilon < 0.12\%$
Peng et al. [18]	$\epsilon = 0.6\%\text{-}1\%$

calculations.

2.5 Roughness Creation and Measurement

An effort by a number of researchers has been made to determine the effect of wall roughness on flow in microchannels. Wall asperities which would have little influence on laminar flow in large scale ducts [27], are important when the channel dimensions become comparable to the roughness.

Table 3 summarizes the reported roughness found in the literature. An ANSI standard [28] provides a method for statistically determining surface roughness, however it is unclear how many, if any, of the authors followed this standard. The roughness can be reported as average roughness which is a average of the absolute value for the asperity height in μm

$$R_a = \frac{1}{L}\int_0^L |z(x)|\, dx \tag{8}$$

or as relative roughness which is commonly defined as:

$$\varepsilon = \frac{R_a}{D_h} \tag{9}$$

It should be noted, however, numerous different approaches were taken to measure and calculate roughness statistically, often without a description of the method in the paper; thus the values cannot be directly compared with confidence.

For circular channels, Jiang et al. [29] used microscopic image-acquisition and processing software to measure the microtube diameter. An image of each end of the glass tube cross-section was obtained using a 100x optical lens. The software took the image and made measurements within a reported accuracy of 1% for diameters as small as 8 μm. For non-circular channels, the same algorithm could also be used to measure channel dimensions but they used a profiler with 0.2 nm resolution instead. The surface roughness of the micro-channel was measured along its length and plotted to show peak-to-valley heights.

Judy et al. [7] used a calibrated scanning electron microscope to measure the diameter of the test specimens under magnifications of 450 to 2200 x. The specimens were sputter-coated with gold to allow easier imaging of the tubes. Eight different diameter measurements, at both the inlet and outlet, were taken at user-defined points for circular tubes and an average diameter was calculated. Similarly, eight different measurements are made at each end of the rectangular channels to determine the width and height.

Pfund et al. [8] obtained the surface profile using a white light interferometer which allowed for non-contact profilometery and for false colour photographs to be taken which illustrated surface topography. The depth of the channels were measured with a microscope which had a stage with micro adjustment. The microscope was focussed on the top surface of the channel initially and then the stage was moved until the bottom surface of the channel came into focus. The depth was determined by how far the stage moved, measured by the micrometer adjustment of the microscope, between seeing the two surfaces in focus. Measurements were made at 9 points along the centerline, and 9 near the wall to provide an average depth.

Kandlikar et al. [14] used acid etching techniques to create test samples with different roughnesses. The tube was filled with acid for 1 minute before emptying. This procedure was then repeated several times and then the channel was soaked for a few hours. To measure the average roughness, the samples were cut longitudinally and a profilometer was used to obtain the roughness profile along the length of the channel. Photographs of the surface were taken with a scanning electron microscope to analyze the roughness qualitatively.

Li et al. [11] used a scanning electron microscope to measure the diameters of the test samples. To measure roughness, the specimens were milled open, and a micrometer was used to measure the peak-to-valley roughness.

Similarly, Celata et al. [15] measured superficial roughness heights from electron microscope images with the average roughness being calculated using a statistical method.

3 ERROR ANALYSIS

In most of the reviewed papers, some error analysis or uncertainty data were provided, but few authors included a comprehensive list of error sources. Table 4 lists the maximum values for the most frequently reported measurement percentage error.

In general, from the estimates provided by the authors, the pressure measurement uncertainties do not vary substantially between all three types of systems. However it can be noted that the authors who used pressure transducers or differential pressure transducers to measure pressure

Table 4. MEASUREMENT UNCERTAINTY

Reference	System Type	Reported Error (%) p	L	Q	D_h
Li et al. [11]	1	1.5	0.1	2.0	2.0
Liu & Garimella [5]	1	0.25	3.90	1.01	-
Wu & Cheng [6]	1	0.68	0.37	1.69	1.83
Mala & Li [16]	2	2.0	0.20	2.0	2.0
Judy et al. [7]	2	0.25	-	-	silica circ.: 2.5 silica sqr.: 2.5 SS: 5.0
Chen et al. [13]	3	2.0	-	5.0	-
Celata et al. [15]	3	-	-	7.0	-
Peng et al. [18],[19]	3	1.5	-	2.5	-

at both the inlet and outlet of open-loop systems, [5; 6; 7], quoted extremely small uncertainties, but Li et al [11] and Mala and Li [16] both calculated greater uncertainty when using only measuring pressure at the inlet and assuming the outlet pressure was atmospheric. Both Chen et al. [13] and Peng et al. [18], who used closed-loop systems, found the pressure measurement using differential pressure transducers or pressure sensors to be very similar to Li et al. [11] and Mala and Li [16].

The lowest uncertainty for flow rate was reported by the four authors who calculated it using a precision scale. The closed loop system appears to be subject to greater uncertainty in flow rate when using in-line flow meters [13; 15; 18].

To provide an overall estimate of the uncertainty associated with each system type, uncertainty in the two most important hydrodynamic flow parameters f, and Re, are compared in Table 5. Alternatively, some authors provided the error associated with the product, $f\,\mathrm{Re}$. In order to provide a common error calculation, in addition to the reported values, a differential error analysis is done by the authors for f, Re, and $f\,\mathrm{Re}$ for each set of uncertainty data.

The differential error is calculated as follows. Given the function, $F = F(x_1, x_2, ..., x_n)$, the absolute uncertainty of F, ω_F, is a function of the uncertainies of the independent variables, $\omega_1, \omega_2, ..., \omega_n$ according to the equation [30],

$$\omega_F = \left[\left(\frac{\partial F}{\partial x_1} \omega_1 \right)^2 + \left(\frac{\partial F}{\partial x_2} \omega_2 \right)^2 + ... + \left(\frac{\partial F}{\partial x_n} \omega_n \right)^2 \right]^{\frac{1}{2}} \tag{10}$$

Further, if the function is only a product of its variables, such as,

$$F = A x_1^a x_2^b ... x_n^m \tag{11}$$

it can be shown that Eq. (11) can be reduced to

$$\frac{\omega_F}{F} = \left[\left(a \frac{\omega_1}{x_1} \right)^2 + \left(b \frac{\omega_2}{x_2} \right)^2 + ... + \left(m \frac{\omega_n}{x_n} \right)^2 \right]^{\frac{1}{2}} \tag{12}$$

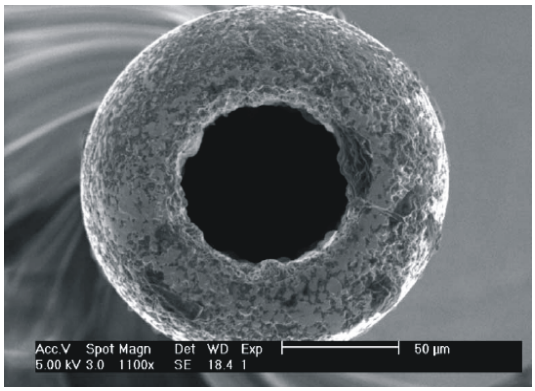

Figure 6. STAINLESS STEEL MICROTUBE, [7]

which gives the percentage error in F [31].

Almost all values calculated from the reported uncertainties are lower than the reported values, and thus other sources of errors which increase the reported overall error must have not been reported in the literature.

Many authors did not report uncertainty in dimensional measurement of Table 4. An uncertainty estimation for dimensions is particularly important given the differential error analysis by Judy et al. [7] into the strong influence of the error in diametric measurement on the uncertainty of the $f\,\mathrm{Re}$ flow parameter. Since the hydraulic diameter appears in the equation raised to the fourth power, see Eq. (4), according to Eq. (12), the error associated with diameter measurements must be multiplied by a factor of four when calculating the error in $f\,\mathrm{Re}$. Thus any small amount of error in this measurement is magnified dramatically. A significant source of error in diameter measurement is the selection of measurement points. Particularly on rough surfaces, such as the SS microtubes used in the study by Judy et al [7], Fig. 6, it is difficult to select points in an unbiased manner around the tube or channel which are representative of the dimensions of the object. Human bias is difficult to quantify, and creates further uncertainty in diameter measurement.

4 SUMMARY AND RECOMMENDATIONS

A review of reported experiments on flow through microchannels and tubes is made with emphasis on how the experiments are conducted.

Upon consideration of the reported information in literature, it is not possible to conclude the method by which the most accurate data can be acquired, however, the following recommendations are made for future experimentation:

- Measurement of cross-sectional dimensions must be

Table 5. PREDICTED VS. CALCULATED UNCERTAINTY

Authors	System Type	Reported Percentage Error f	Re	fRe	Calculated Percentage Error f	Re	fRe
Li et al. [11]	1	-	-	10.0	2.5	2.0	8.38
Liu & Garimella [5]	1	11.8	10.5	-	3.91	-	4.04
Wu & Cheng [6]	1	-	-	11.0	1.99	1.83	7.55
Mala & Li [16]	2	9.2	3.0	-	2.84	4.92	8.49
Judy et al. [7]	2	-	-	silica circ.: 15.0 silica sqr.: 11.4 SS: 21.4	silica circ.: 2.51 silica sqr.: 2.51 SS: 5.01	silica circ.: 2.5 silica sqr.: 2.5 SS: 5.0	silica circ.: 10.0 silica sqr.: 10.0 SS: 20.0
Chen et al. [13]	3	5.4	10.5	-	2.0	-	5.39
Celata et al. [15]	3	7.0	5.0	-	1.75	7.08	7.08
Peng et al. [18],[19]	3	10.0	8.0	-	1.5	-	2.92

done as accurately as possible, as it has a great effect on the error in f, Re and $f\,\mathrm{Re}$ calculations.

- Roughness should be measured, calculated and reported as per standards such as [28] to allow for accurate comparison between measurements. Furthermore, studies should be conducted into determining the effects of wall roughness on microflow.
- The entrance or developing flow region should be considered when determining the test channel L/D_h ratio.

ACKNOWLEDGMENT

The authors gratefully acknowledge the financial support of the Centre for Microelectronics Assembly and Packaging, CMAP and the Natural Sciences and Engineering Research Council of Canada, NSERC.

REFERENCES

[1] G. L. Morini, "Single-phase convective heat transfer in microchannels: A review of experimental results," *International Journal of Thermal Sciences*, vol. 43, pp. 631–651, 2004.

[2] N. T. Obot, "Toward a better understanding of friction and heat/mass transfer in microchannels- a literature review," *Microscale Thermophysical Engineering*, vol. 6, pp. 155–173, 2002.

[3] C. B. Sobhan and S. V. Garimella, "A comparative analysis of studies on heat transfer and fluid flow in microchannels," *Microscale Thermophysical Engineering*, vol. 5, no. 4, pp. 293–311, 2001.

[4] I. Papautsky and T. Ameel, "A review of laminar single-phase flow in microchannels," *ASME, Proceedings of Int. Mech. Eng Congress Expos Proc (IMECE) 2001, ASME, New York*, vol. 2, pp. 3067–3075, 2001.

[5] D. Liu and S. V. Garimella, "Investigation of liquid flow in microchannels," *Journal of Thermophysics and Heat Transfer*, vol. 18, no. 1, pp. 65–72, 2004.

[6] H. Y. Wu and P. Cheng, "Friction factors in smooth trapezoidal silicon microchannels with different aspect ratios," *International Journal of Heat and Mass Transfer*, vol. 46, pp. 2519–2525, 2003.

[7] J. Judy, D. Maynes, and B. W. Webb, "Characterization of frictional pressure drop for liquid flows through microchannels," *International Journal of Heat and Mass Transfer*, vol. 45, pp. 3477–3489, 2002.

[8] D. Pfund, D. Rector, A. Shekarriz, A. Popescu, and J. Welty, "Pressure drop measurements in a microchannel," *Fluid Mechanics and Transport Phenomena*, vol. 46, no. 8, pp. 49–60, 2000.

[9] D. B. Tuckerman and R. F. W. Pease, "High-performance heat sinking for vlsi," *IEEE Electron Device Letters*, no. 5, pp. 126–129, 1981.

[10] J. Pfahler, J. Harley, H. Bau, and J. Zemel, "Liquid transport in micron and submicron channels," *Sensors and Actuators*, pp. 431–434, 1990.

[11] Z. Li, D. Du, and Z. Guo, "Experimental study on flow characteristics of liquid in circular microtubes," *Microscale Thermophysical Engineering*, vol. 7, no. 3, pp. 253–265, 2003.

[12] L. Zhang, J. M. Koo, L. Jiang, M. Asheghi, K. E. Goodson, J. G. Santiago, and T. W. Kenny, "Measurements and modeling of two-phase flow in microchannels with nearly constant heat flux boundary conditions," *Journal of Microelectromechanical Systems*, vol. 11, no. 1, 2002.

[13] Y. T. Chen, S. W. Kang, W. C. Tuh, and T. H. Hsiao, "Experimental investigation of fluid flow and heat transfer in microchannels," *Tamkang Journal of Science and Engineering*, vol. 7, no. 1, 2004.

[14] S. G. Kandlikar, S. Joshi, and S. Tian, "Effect of channel roughness on heat transfer and fluid flow characteristics at low reynolds numbers in small diameter tubes," *Proceedings of the National Heat Transfer Conference*, vol. 2, pp. 1609–1618, 2001.

[15] G. P. Celata, M. Cumo, M. Guglielmi, and G. Zummo, "Experimental investigation of hydraulic and single phase heat transfer in 0.130 mm capillary tube," *Eng.*

6, Microscale Thermophys, pp. 85–97, 2002.

[16] G. M. Mala and D. Q. Li, "Flow characteristics of water in microtubes," *International Journal of Heat and Fluid Flow*, vol. 20, no. 2, pp. 142–148, 1999.

[17] P. Gao, S. L. Person, and M. Favre-Marinet, "Scale effects on hydrodynamics and heat transfer in two-dimensional mini and microchannels," *International Journal of Thermal Sciences*, vol. 41, pp. 1017–1027, 2002.

[18] X. F. Peng and G. P. Peterson, "Convective heat transfer and flow friction for water flow in microchannel structures," *Internation Journal Heat Mass Transfer*, vol. 39, no. 12, pp. 2599–2608, 1996.

[19] X. F. Peng, G. P. Peterson, and B. X. Wang, "Frictional flow characteristics of water flowing through rectangular microchannels," *Experimental Heat Transfer*, vol. 7, no. 4, pp. 249–264, 1994.

[20] S. S. Hsieh, C. Y. Lin, and C. F. Huang, "Liquid flow in a micro-channel," *Journal of Micromechanics and Microengineering*, vol. 14, pp. 436–445, 2004.

[21] B. Xu, K. Ooi, N. Wong, and W. Choi, "Experimental investigation of flow friction for liquid flow in microchannels," *Int. Comm. Heat Transfer*, vol. 27, no. 8, pp. 1165–1176, 2000.

[22] W. Owahib and B. Palm, "Experimental investigation of single-phase convective heat transfer in circular microchannels," *Experimental Thermal and Fluid Science*, vol. 28, pp. 105–110, 2004.

[23] T. M. Adams, S. I. Abdel-Khalik, S. M. Jeter, and Z. H. Qureshi, "An experimental investigation of single-phase forced convection in microchannels," *Int. J. Heat Mass Transfer*, vol. 41, no. 6-7, pp. 851–857, 1998.

[24] W. Qu and I. Mudawar, "Transport phenomena in two-phase micro-channel heat sinks," *Proceedings of ASME International Mechanical Engineering Conference Exposition, New Orleans, Louisiana*, 2002.

[25] I. E. Idelchik, *Handbook of Hydraulic Resistance 3rd Edition*. Boca Raton, FL, USA: CRC Press Inc., 1994.

[26] F. M. White, *Fluid Mechanics, 3rd Ed.* New York: McGraw-Hill, Inc., 1994.

[27] L. F. Moody, "Friction factors for pipe flow," *Trans. ASME*, vol. 66, pp. 671–684, 1944.

[28] in *Surface Texture: surface Roughness, Waviness and Lay*, American Society of Mechanical Engineers: ANSI B46.1, 1985.

[29] X. N. Jiang, Z. Y. Zhou, X. Y. Huang, and C. Y. Liu, "Laminar flow through microchannels used for microscale cooling systems," *IEEE CPMT Electronic Packaging Technology Conference*, pp. 119–122, 1997.

[30] M. Bahrami, *Modeling of Thermal Joint Resistance for Rough Sphere-Flat Contact in a Vacuum*. PhD thesis, University of Waterloo, Dept. of Mech. Eng., Waterloo, Canada, 2004.

[31] A. J. Wheeler and A. R. Ganji, *Introduction to Engineering Experimentation, 2nd Ed.* Upper Saddle River, NJ: Pearson Education, Inc., 2004.